

Single-track Model for Lane Keeping and Path Tracking Control

Dynamic model, simulation and results analysis for various operative conditions



**Politecnico
di Torino**

Sofia Longo S310183

Gabriele Martina S310789

Luigi Maggipinto S319874

Technologies for Autonomous Vehicles A.Y. 2023/2024

Contents

1 System Model	2
2 Manoeuvres	2
3 State feedback control	2
3.1 Pole placement	3
4 Gains	6
4.1 Curvature Gain	7
4.2 Lateral Acceleration Gain	8
4.3 Yaw rate Gain	8
4.4 Side slip angle Gain	8
5 Rear Axle Cornering Stiffness Variation	9
6 Vehicle response variables	12
7 Notes	12

1 System Model

This report presents a **single-track model** of a vehicle and discusses its behaviour along different curvature profiles.

The system is modelled through a linear state-space representation formulated as:

$$\dot{x}(t) = Ax(t) + B_1\delta(t) + B_2\dot{\psi}_{des}(t)$$

$$y(t) = Cx(t), \quad C = I_4,$$

where the states variables are the lateral deviation (e_1), the relative yaw angle (e_2) and their first derivatives:

$$x_1 = e_1(t) = y(t) - y_{cl}(t)$$

$$x_2 = \dot{e}_1(t) = v_y(t) + \bar{V}_x e_2(t)$$

$$x_3 = e_2(t) = \psi(t) - \psi_{des}(t)$$

$$x_4 = \dot{e}_2(t) = \dot{\psi}(t) - \dot{\psi}_{des}(t)$$

where $y_{cl}(t)$ is the position of the center line of the lane along the y-axis; $\dot{\psi}_{des}(t)$ is the desired yaw rate profile; and \bar{V}_x is the constant module of the vehicle velocity.

Starting from e_1 we get the lateral component of the velocity vector, and along with \bar{V}_x we can obtain the side slip angle β . Also, through the inverse formula of Ackermann angle δ we get the curvature K_L .

All the other variables (such as $\alpha_R, \alpha_F, a_x, a_y, \dot{\psi}, \dot{\beta}$) are evaluated through directed formulas and can be observed in the Simulink project.

2 Manoeuvres

We include three possible manoeuvres that can be performed in order to evaluate the control strategy. For each one, the trajectory that the vehicle follows is visualised through plots in birds-eye-view:

- Ramp steer (Fig.1a),
- Sine sweep, to emulate skidpad (Fig.1b),
- Drift steer (Fig.1c),
- Obstacle avoidance with lane re-enter (Fig.1d).

From the manoeuvre curvature profile we get the Ackermann steering angle and map it to the curvature of our desired trajectory. This is injected into our controller.

3 State feedback control

A linear state feedback controller is designed to stabilize the vehicle dynamics and ensure it keeps the lane and follows the desired path accurately.

Inputs to the plant are the steering angle δ and the desired yaw rate $\dot{\psi}_{des}$.

These are built such that:

$$\dot{\psi}_{des} = K_L \cdot \bar{V}_x$$

$$\delta = \delta_{ff} - Kx(t) = K_L K_{ff} - Kx(t).$$

To better understand our system's behaviour we briefly analyse how the roots vary with vehicle speed in open loop, focusing on the understeering case. The root locus is evaluated starting from a very low velocity of 1 km/h up to 300 km/h. As shown in Fig.2a, these roots are real at very low values of velocity, where they show a high natural frequency (Fig.2b). This means that changes in the input are rapidly reflected in the output. As the vehicle speed increases, they become couples of complex conjugate poles where the damping ratio progressively decreases (Fig.2c), as does the system's capability to attenuate oscillations.

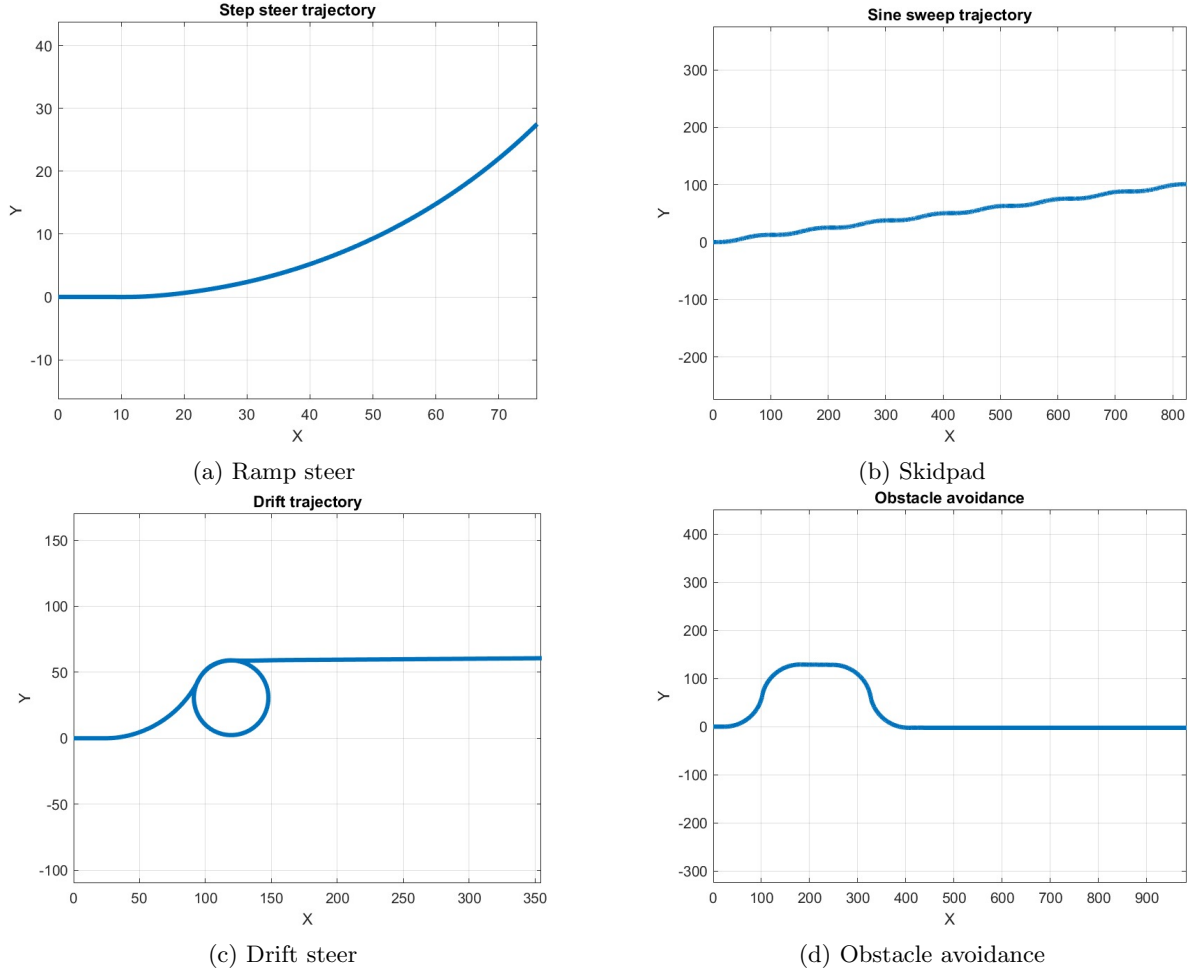


Figure 1: Manoeuvres

Furthermore, by examining the Bode plots of the aforementioned system (Fig.3a and Fig.3b) , we can conclude that it behaves like a low-pass filter attenuating all frequencies higher than 10Hz. This applies from both input signals (δ steering wheel angle and ψ desired yaw rate), to both output responses (e_1 deviation from central line and e_2 offset from the desired yaw angle).

3.1 Pole placement

The action of control takes place, firstly, in **feedforward** through the design of K_{ff} which helps by minimizing the steady-state error by accounting for predictable dynamics of the vehicle. Secondly, the **feedback** loop closes over vector K that performs a pole placement to impose the eigenvalues that dictate the dynamics and therefore stabilize the system, guaranteeing convergence to the desired trajectory.

We can observe from Fig.4, the contributions of the feedforward and feedback steering angles during a standard simulation. It is noticeable that, in a quasi-steady state scenario, the contribution of K_{ff} in absolute terms is significantly larger than that of K. Furthermore, it is evident that the feedback component functions, merely, as a corrective term in transient condition. This occurs because, during the selection of the poles for K, we opted to place them in the negative region but with a low magnitude. If we had chosen poles with a higher magnitude, we would have achieved vehicle stability at an even faster rate. However, this would have caused the vehicle to experience severe vibrations during the steering phase, due to the increased contribution from the feedback component.

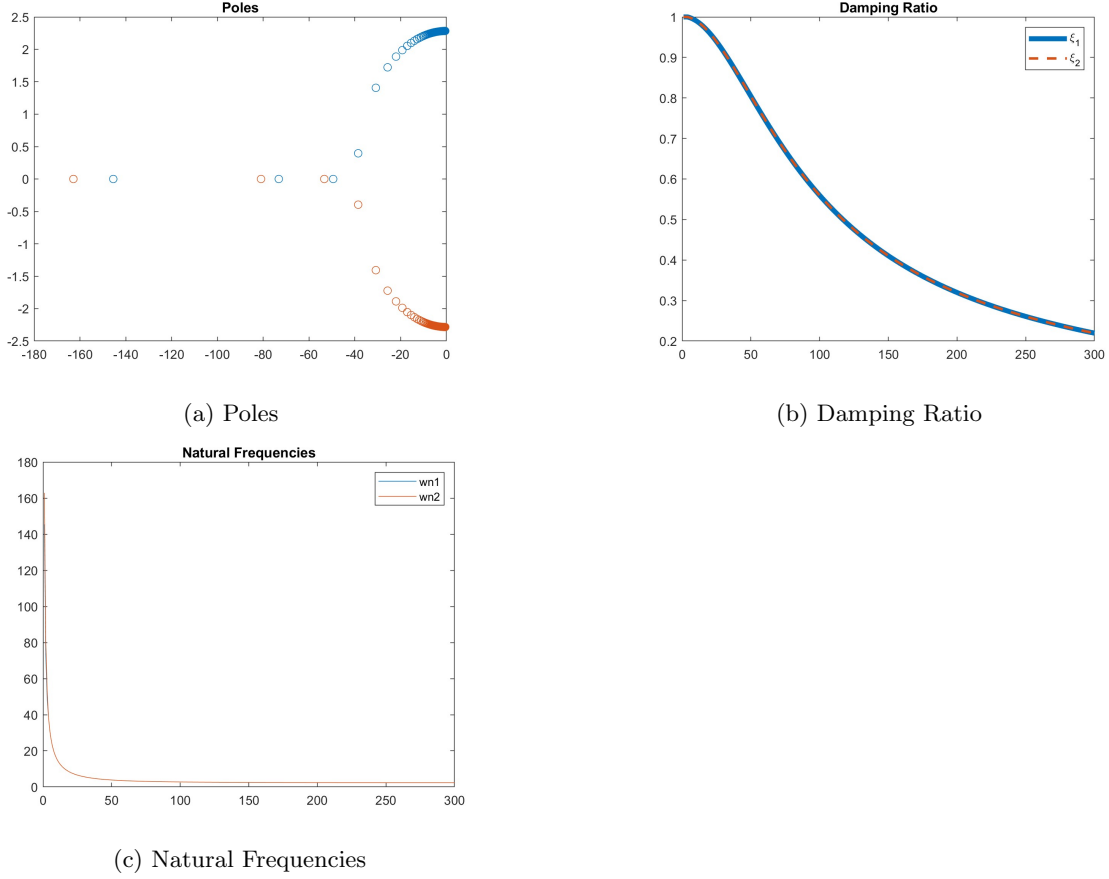


Figure 2: Root locus

Hence, the aim is stabilizing the system dynamics by imposing all 4 eigenvalues of matrix A through a simple pole placement technique such that the new dynamics is dictated by $\bar{A} = A - KB_1$. In order to stabilise the system these must be chosen with $\Re(\lambda_i) < 0$. If we select only real negative poles, the system's response will exhibit no oscillations but will be significantly slower. Conversely, by imposing two complex conjugate poles with a small real part in magnitude and a sufficiently high damping ratio, we can compensate for the oscillatory response while retaining the advantages of a rapid settling time. Through some experiments we have asserted that the best control action is indeed obtained when setting the first 2 poles as complex conjugates with negative and relatively small real part, and the other 2 as real and negative, also small in magnitude.

In fact, if we consider a **step steer** with 30 km/h speed, and choose four real poles such as $[-1, -2, -3, -4]$ the system is capable of driving the first state to zero within $10s$, achieving an accuracy margin of 10^{-4} , and the second state to zero with a margin of 10^{-2} , which is still good performance yet not particularly satisfying (Fig.5).

Slightly better results are obtained when choosing $[-2 + 2i, -2 - 2i, -5, -6]$ as poles. In Fig.6 we can see how the peak values are much smaller and the transient is quicker. Even better results are achieved when the poles are $[-23 + 6i, -23 - 6i, -9, -12]$ both in terms of transient and peak values (Fig.7); however, due to the increase in the magnitude of poles, the feedback contribution becomes higher than the feedforward contribution that, as previously discussed, causes some unbearable oscillations in the steady-state phase (Fig. 8).

Therefore, we have chosen $[-2 + 2i, -2 - 2i, -5, -6]$ for further simulations.

The plots in Fig.9 represent the system's responses to a step steer in terms of side slip angle β and yaw rate r when we choose $[-23 + 6i, -23 - 6i, -9, -12]$ as poles. The characteristics of these responses are well represented by parameters like rise time, $t_r(10\% - 90\%)$, and settling time at 5%,

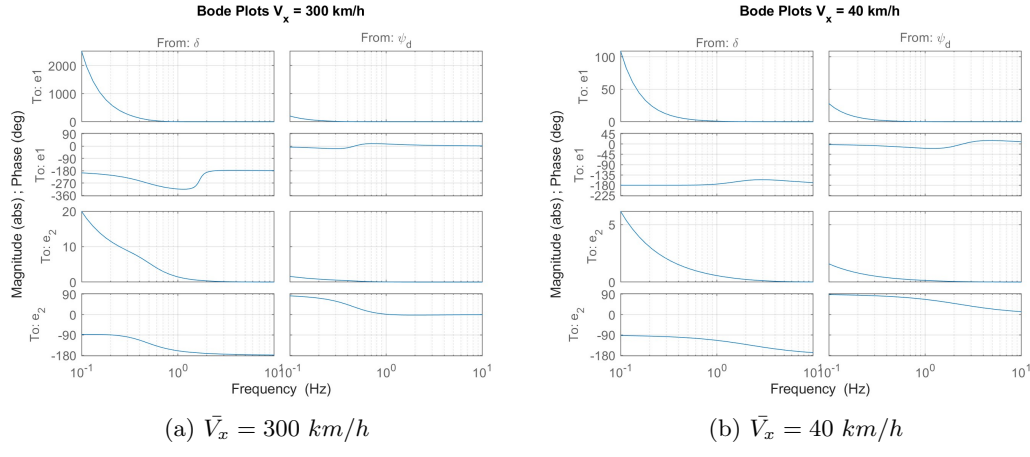


Figure 3: Bode Plots

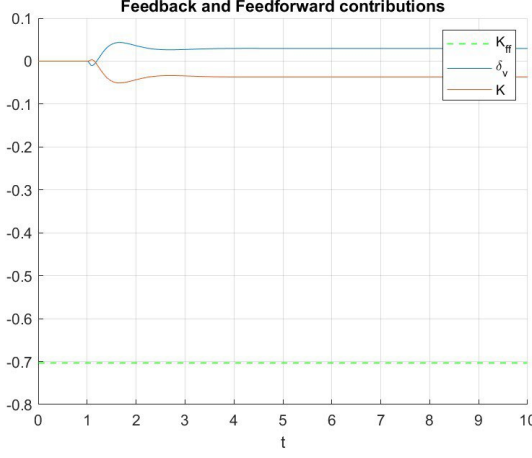


Figure 4: Feedback and Feedforward contributions

$t_{s,5\%}$. Note that we do not have an overshoot, the response converges directly to the final value.

- β :

$$t_r(10\% - 90\%) = 0.25s$$

$$t_{s,5\%} = 0.43s$$

- $\dot{\psi}$:

$$t_r(10\% - 90\%) = 0.4s$$

$$t_{s,5\%} = 0.5s$$

On the contrary, when analysing the same curves for another set of poles ($[-2 + 2i, -2 - 2i, -5, -6]$, Fig.10), we immediately observe a deterioration in performance.

- β :

$$t_r(10\% - 90\%) = 2.11s$$

$$t_{s,5\%} = 3.45s$$

$$\hat{s} = 30\%$$

- $\dot{\psi}$:

$$t_r(10\% - 90\%) = 0.04s$$

$$t_{s,5\%} = 3.35s$$

$$\hat{s} = 430\%$$

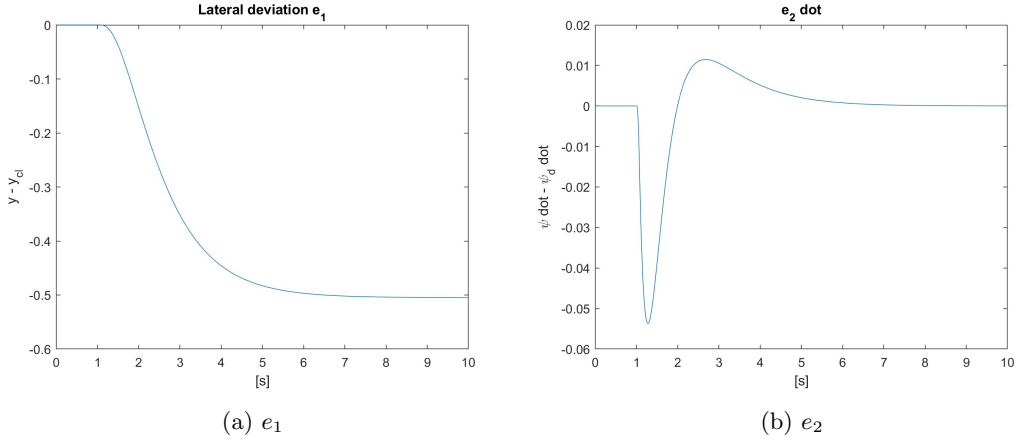


Figure 5: Step steer, $30\text{km}/\text{h}$, poles = $[-1, -2, -3, -4]$

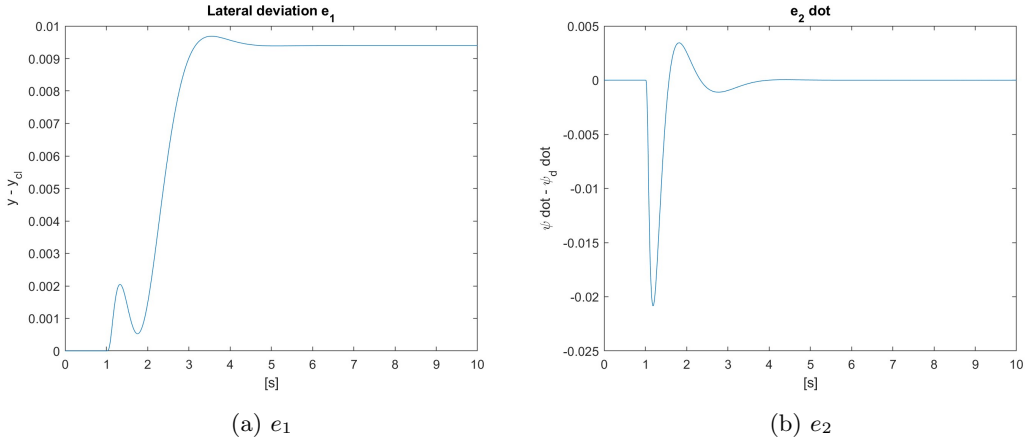


Figure 6: Step steer, $30\text{km}/\text{h}$, poles = $[-2 + 2i, -2 - 2i, -5, -6]$

There is a pronounced transient response and a significant overshoot, particularly in $\dot{\psi}$ where the overshoot reaches four times the final value. This confirms that the previous choice of poles was more effective, yet not usable for the discussed reasons, and the second set of poles has some visible limitations.

Fig.11 shows the tracking errors obtained from applying the same controller to an obstacle avoidance maneuver with lane re-entry starting at a speed of $80\text{ km}/\text{h}$. The controller exhibits quite good tracking performance: peaks correspond to the variations in the reference curvature profile; the response quickly readjusts to the new command value.

On the other hand, it is immediately noticeable from Fig.12 that the tracking capabilities are significantly poorer with the choice of all real poles.

When testing the drift manoeuvre we get an analogous behaviour (Fig.13).

A different case is the sine sweep (skidpad, Fig.14), where lateral deviation and errors in desired yaw rate tracking persistently oscillate without reaching zero. The system keeps reacting to some transient and never achieves perfect convergence to the reference, at least with this type of control. Nevertheless, it significantly mitigates the magnitude of the deviation and generally maintains lane alignment.

4 Gains

Here we analyse **gains** that are ratios calculated in steady state cornering conditions between a variable relevant to the cornering response of the car and the steering input δ .

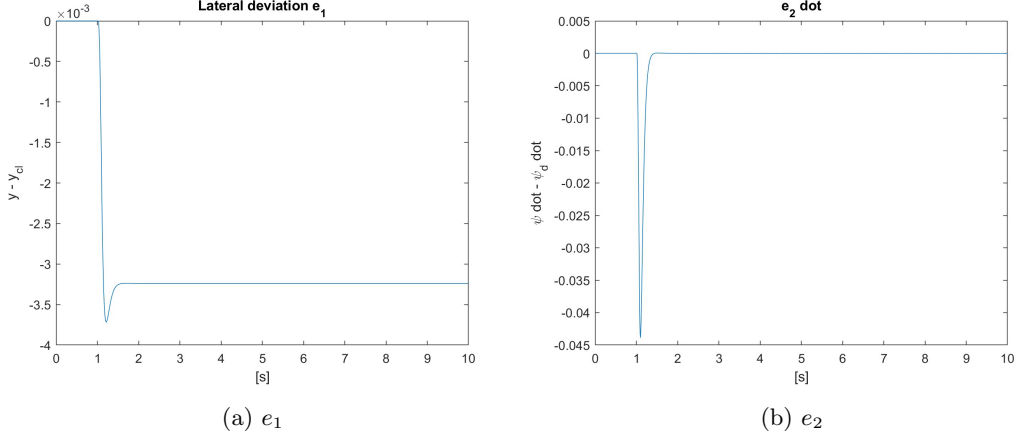


Figure 7: Step steer, 30km/h, poles = $[-23 + 6i, -23 - 6i, -9, -12]$

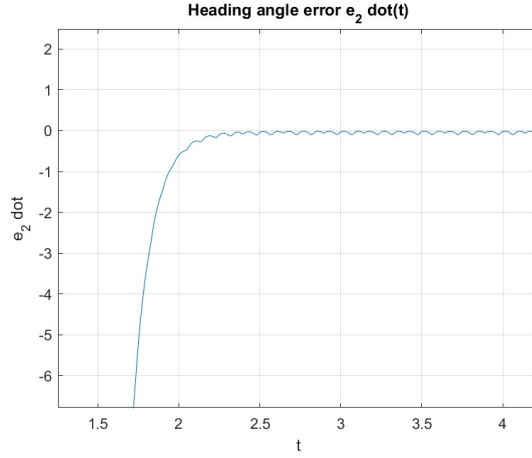


Figure 8: Oscillations with poles $[-23 + 6i, -23 - 6i, -9, -12]$

In order to visualise these metrics we calculate them by varying the vehicle speed and plotting the gain's behaviour.

4.1 Curvature Gain

The response to steer angle δ in terms of curvature KL is given by:

$$\frac{\rho}{\delta} = \frac{1}{R\delta} = \frac{1}{L + KV^2}$$

and its trend is shown in Fig.15a where we consider all types of steering: oversteering, neutral steering and understeering by varying the rear axle cornering stiffness C_R respectively as $[1e5, 1.04e5, 11.4e5]$. We can notice that in the first case, due to the negative value of K , the gain grows exponentially with the increase in speed until it reaches the critical velocity $V_{cr} = \sqrt{\frac{-L}{K}}$ (highlighted with a green dashed line), which causes an instability when

$$L + KV^2 = 0$$

Consequently, in the neutral steering case, the gain remains steady because of the null value of K , and the understeering curve, as expected, decreases slowly with the velocity enhancement.

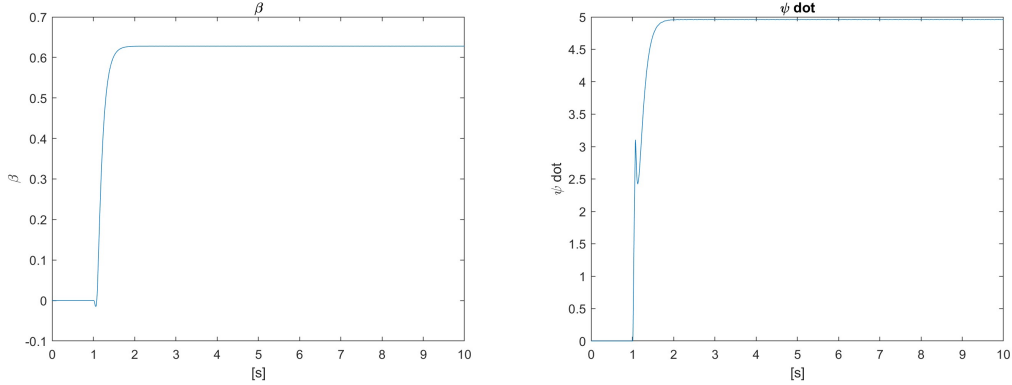


Figure 9: Step steer response in β and $\dot{\psi}$ with poles $[-23 + 6i, -23 - 6i, -9, -12]$

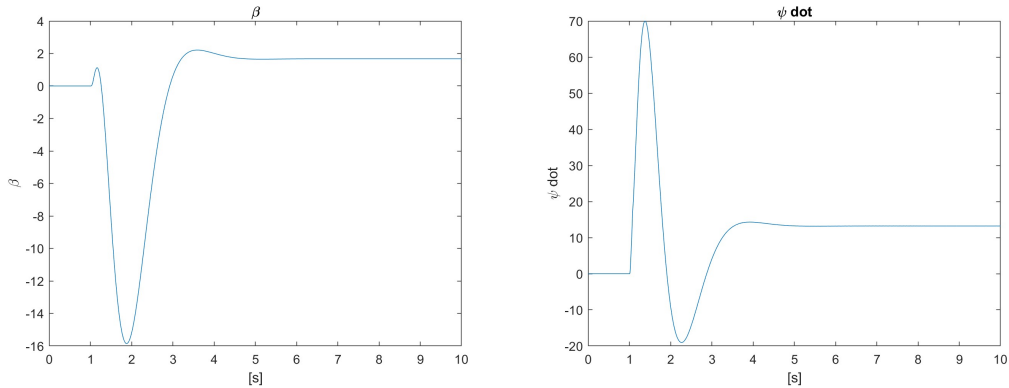


Figure 10: Step steer response in β and $\dot{\psi}$ with poles $[-2 + 2i, -2 - 2i, -5, -6]$

4.2 Lateral Acceleration Gain

The response to steer angle δ in terms of lateral component of the acceleration a_y is (Fig.15b):

$$\frac{a_y}{\delta} = \frac{V^2}{R\delta} = \frac{V^2}{L + KV^2}$$

As in the case of Curvature gain, if $K < 0$ (oversteering), the growth is exponential up to the critical velocity. Conversely, in the case of neutral steering, the trend is not constant as it depends quadratically on the increase in speed. When $K > 0$ (understeering), the gain tends to increase, although more slowly.

4.3 Yaw rate Gain

The response to steer angle δ in terms of yaw rate $\dot{\psi}$ is (Fig.15c):

$$\frac{\dot{\psi}}{\delta} = \frac{V}{L + KV^2}$$

Here, the behavior of the gain is similar to what was observed previously, but with a more damped growth due to the linear dependence on speed.

4.4 Side slip angle Gain

Finally, the response to steer angle δ in terms of side slip angle β is (Fig.15d):

$$\frac{\beta}{\delta} = a_r \left(1 - \frac{ma_f V^2}{a_r LC_r}\right) \frac{1}{L + KV^2}$$

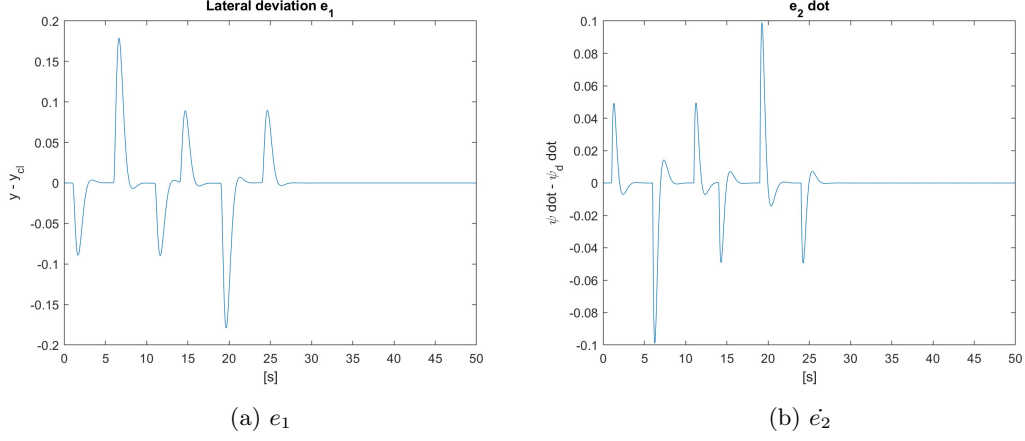


Figure 11: Obstacle avoidance, $80\text{km}/\text{h}$, poles = $[-2 + 2i, -2 - 2i, -5, -6]$

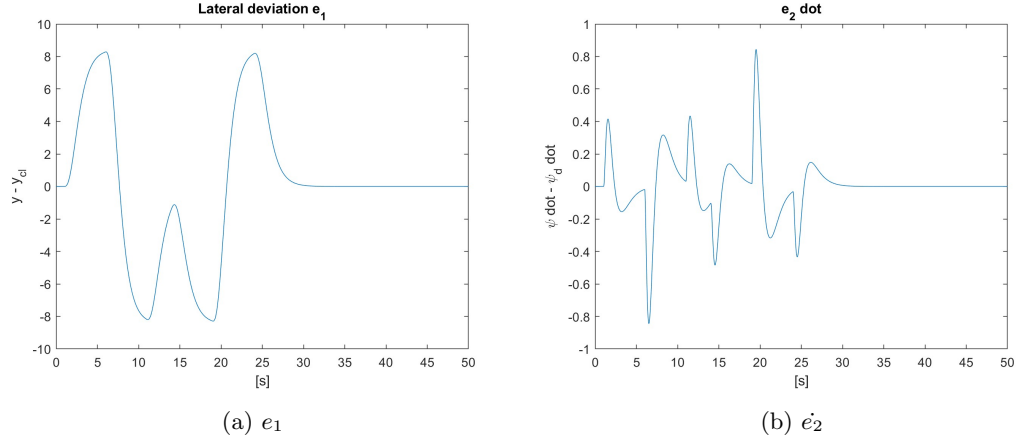


Figure 12: Obstacle avoidance, $80\text{km}/\text{h}$, poles = $[-1, -2, -3, -4]$

The behavior of this gain is opposite to what was observed in the previous computations. The trend is decreasing in all three steering cases.

5 Rear Axle Cornering Stiffness Variation

In the initial conditions, an understeering situation is observed. It has been noted that, since the vehicle's center of mass is not precisely in the middle, it is not sufficient to make the cornering stiffness of the rear axle (C_r) equal to that of the front axle (C_f), to achieve neutral steering. Similarly, increasing C_r , compared to C_f , does not necessarily guarantee oversteering. Starting from $C_f = 1.2e5$, for oversteering to occur, C_r must be less than or equal to $1.04e5$, while neutral steering is achieved if $C_r \approx 1.04e5$, as illustrated in the figure 16a.

By varying C_r and consequently changing the type of steering, the profile of the control input K_{ff} varies accordingly:

$$K_{ff} = \left[\frac{m_v v_x^2}{L} \left(\frac{a_r}{C_f} - \frac{a_f}{C_r} + \frac{a_f}{C_r} k_3 \right) + L - a_r k_3 \right]$$

where a_r , a_f , L , k_3 are, respectively, the distance of rear and front axles w.r.t. CG , the wheelbase and the third component of the feedback control vector K .

In particular, in the case of oversteering (with a reduction in C_r), K_{ff} increases and vice versa, as highlighted in the image 16b.

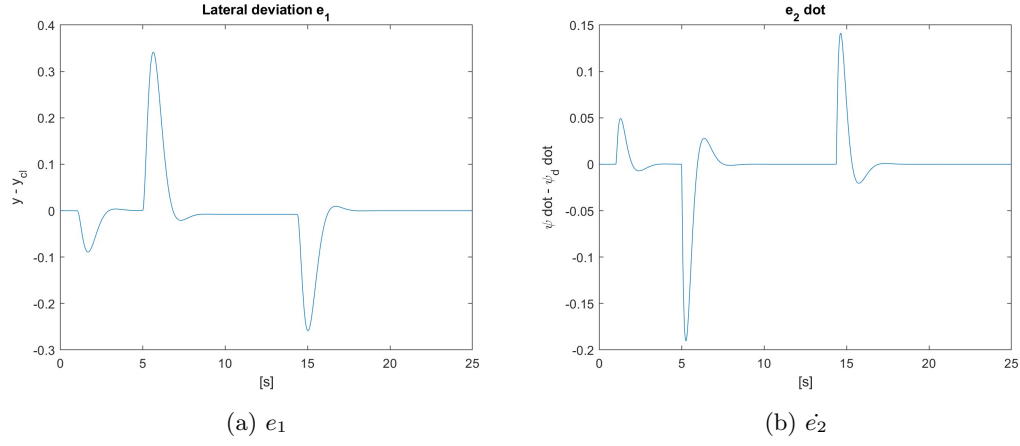


Figure 13: Drift, $80\text{km}/\text{h}$, poles = $[-2 + 2i, -2 - 2i, -5, -6]$

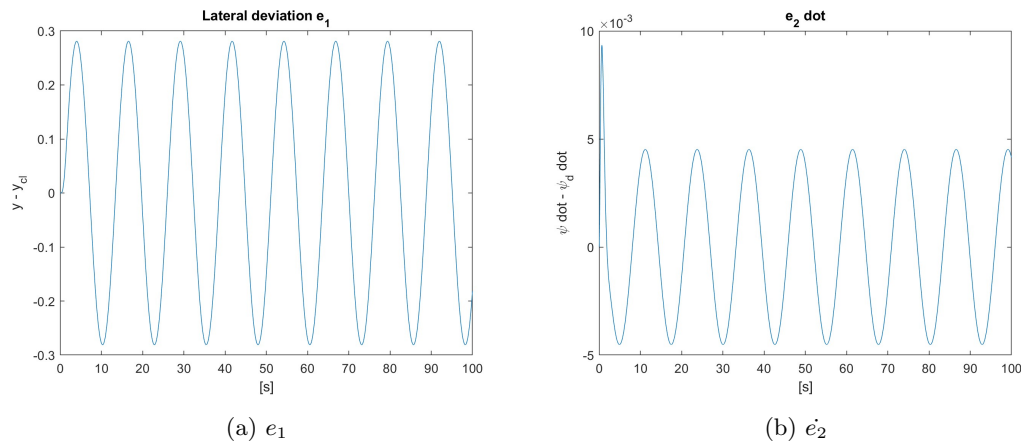


Figure 14: Sine sweep, $30\text{km}/\text{h}$, poles = $[-2 + 2i, -2 - 2i, -5, -6]$

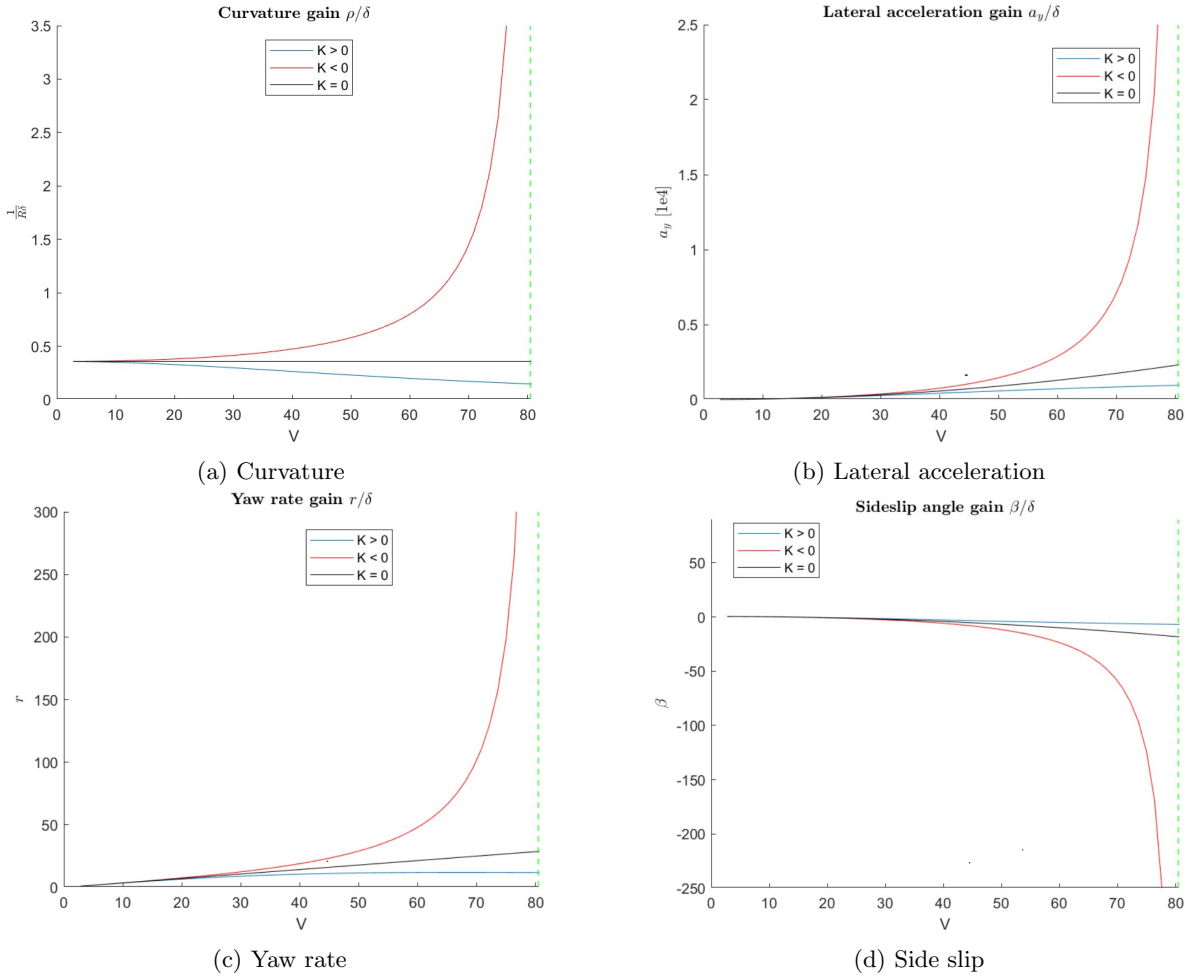


Figure 15: Gains

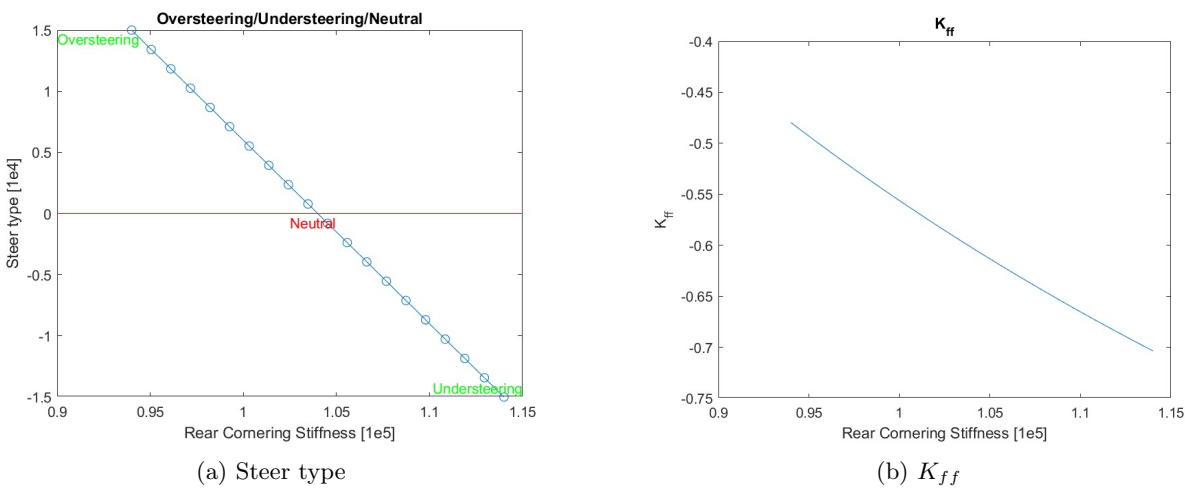


Figure 16: CR and K_{ff}

6 Vehicle response variables

In the context of analyzing and controlling the steering behavior of a single track model, given a constant velocity ($Vx = 30km/h$) and a reference maneuver (Ramp steer), the main control variables to consider are:

- **Lateral error** $e_1(t)$: modeling the controller involves attempting to reduce this error to zero (or, more generally, to minimize it as much as possible) so that the vehicle can keep the lane. To achieve this and stabilize the system, four negative poles were used after some tuning: $[-2 + 2i, -2 - 2i, -6, -5]$ (Fig. 17a).
- **Heading angle error** $\dot{e}_2(t)$: controlling and minimizing this error is essential to keep the vehicle on the desired trajectory. A high error could cause the vehicle to deviate from the intended path (Fig. 17b).
- **Yaw rate** $\dot{\psi}$: the angular velocity of the vehicle's rotation around its vertical axis passing through the center of gravity G (Fig. 17c).
- **Sideslip angle** β : the ratio between the lateral component v of the velocity vector and its longitudinal component u (Fig. 17d).

$$\beta = \frac{v}{u}$$

- **Lateral acceleration** a_y : y-component of the vehicle acceleration (Fig. 17e).
- **Front and rear slip angles** α_f, α_r : They are defined as the angle between the direction in which a wheel is actually oriented and the direction in which it is actually moving. In other words, they represent the difference between the ideal path of the wheel (the direction in which it is steered) and the direction in which the wheel is actually moving.

$$\alpha_f = \delta_v \tau_s - \frac{Vx_x + \dot{\psi} a_f}{Vx_y}$$

$$\alpha_r = \delta_v \tau_2 - \frac{Vx_x - \dot{\psi} a_r}{Vx_y}$$

where τ_s is the steering ratio for the front tyre; $\tau_2 = \chi \tau_s = 0.1 \tau_s$ is the steering ratio for the rear tyre; and δ_v is the controlled input of the system. Fig. 17f shows, as we would expect for an understeering vehicle, that the front tyre slip angle is bigger than the rear one.

7 Notes

- Introducing a **PI controller** allows the system to accurately follow a setpoint value over time, correcting any offset errors. Simple pole placement does not necessarily guarantee the elimination of steady-state error. The PI controller can improve the transient response of the system by reducing overshoot and settling time, through appropriate tuning of the proportional and integral gains. Therefore, an integral control contribution would help to improve performance.
Finally, this type of control could lead to better tracking performance also in the manoeuvre of the sine sweep.
- The presence of a **pure time delay** of $0.01s$ in the generation of the feedforward control input allows simulating the transmission delay of information from the road or vehicle path detection system to the control unit managing the system's motion. In practice, this delays the signal generation and, consequently, the control action by $0.01s$.

